Steric and Chelating Ring Concerns on the L-Lactide Polymerization by Asymmetric β-Diketiminato Zinc Complexes

Wan-Jung Chuang,[a] Hsing-Yin Chen,[a] Wei-Ting Chen,[a] Heng-Yi Chang,[a] Michael Y. Chiang,[ab] Hsuan-Ying Chen,*[a] Sodio C. N. Hsu*[a]

[a]*Department of Medicinal and Applied Chemistry, Kaohsiung Medical University, Kaohsiung 807, Taiwan*

[b]*Department of Chemistry, National Sun Yat-Sen University, Kaohsiung 804, Taiwan*

Table S1. Crystal Data and Structure Refinement Parameters

	L^1H	**1** [$L^1ZnEt]_2$	**2** [L^2ZnEt]	**3** [$L^3ZnEt]_2$	**4** [L^4ZnEt]
empirical formula	$C_{23} H_{31} N_3$	$C_{44}H_{58}N_6Zn_2$	$C_{23}H_{31}N_3Zn$	$C_{50}H_{70}N_6Zn_2$	$C_{26}H_{37}N_3Zn$
formula weight	349.51	801.70	414.88	885.86	456.96
T (K)	200(2)	200(2)	200(2)	200(2)	200(2)
cystal size (mm^3)	0.68 x 0.55 x 0.08	0.23 x 0.19 x 0.06	0.18 x 0.17 x 0.08	0.35 x 0.31 x 0.24	0.20 x 0.13 x 0.05
crystal system	Triclinic	triclinic	monclinic	triclinic	monclinic
space group	P -1	P-1	P2(1)/n	P-1	P2(1)/n
a (Å)	9.3914(8)	8.137(9)	10.6411(6)	9.6519(7)	8.8377(8)
b (Å)	10.7363(10)	9.251(10)	14.0394(7)	9.7012(7)	34.635(3)
c (Å)	11.2888(9)	14.151(15)	14.2237(8)	14.3904(11)	9.0028(9)
α (deg)	99.922(4)	79.83(2)	90	76.206(3)	90
β (deg)	100.271(4)	78.73(2)	97.421(2)°.	88.607(3)	118.1850(10)°
γ (deg)	101.376(5)	76.91(2)	90	63.321(3)	90
V ($Å^3$)	1072.30(16)	1007.6(18)	2107.1(2)	1163.94(15)	2428.9(4)
Z	2	1	4	1	4
D_{calcd} (g cm^{-3})	1.082	1.321	1.308	1.264	1.250
μ (mm^{-1})	0.064	1.229	1.177	1.070	1.028
reflns mcasd/indep	7157 / 3667	6025/3483	11629/3726	9718/4053	15366/4249
data/rcstraints/params	3667 / 0 / 235	3483/0/235	3726/0/244	4053/0/262	4249/0/271
GOF	1.075	0.997	1.042	1.037	1.025
R_{int}	0.0388	0.0671	0.0337	0.0188	0.0398
R_1 [$I > 2\sigma$](all data)	0.0886 (0.2536)	0.0866 (0.2035)	0.0374(0.0982)	0.0310 (0.0824)	0.0437(0.0979)
R_w [$I > 2\sigma$](all data)	0.1011 (0.2630)	0.1526(0.2400)	0.0493(0.1044)	0.0339(0.0842)	0.0625(0.1053)
max. peak/hole (e^-/ $Å^3$)	0.450/ -0.500	1.185/ -1.130	0.544/ -0.400	0.653/ -0.606	0.429/ –0.365

Table S2 Kinetic study of *L*-lactide polymerization with various Zn complexes

	1	2	3	4
Time (min)	Conv. of *L*-lactide			
1	0.32	0.38		
2	0.49	0.41		
4	0.67	0.51		
8		0.71		
12	0.97			
15	0.99	0.84		
20			0.39	
30			0.45	
37				0.45
60			0.54	
80			0.60	
87				0.55
107				0.58
127				0.61
160				0.65
190				0.68
220				0.71

$[LA]_0/[$**Zn** $+ BnOH] = 100$; $[LA]_0 = 1.00$ M in CH_2Cl_2 for **1-3** or $[LA]_0/[$**Zn** $+ BnOH] = 50$; $[LA]_0 = 1.32$ M in $CDCl_3$ for **4.**

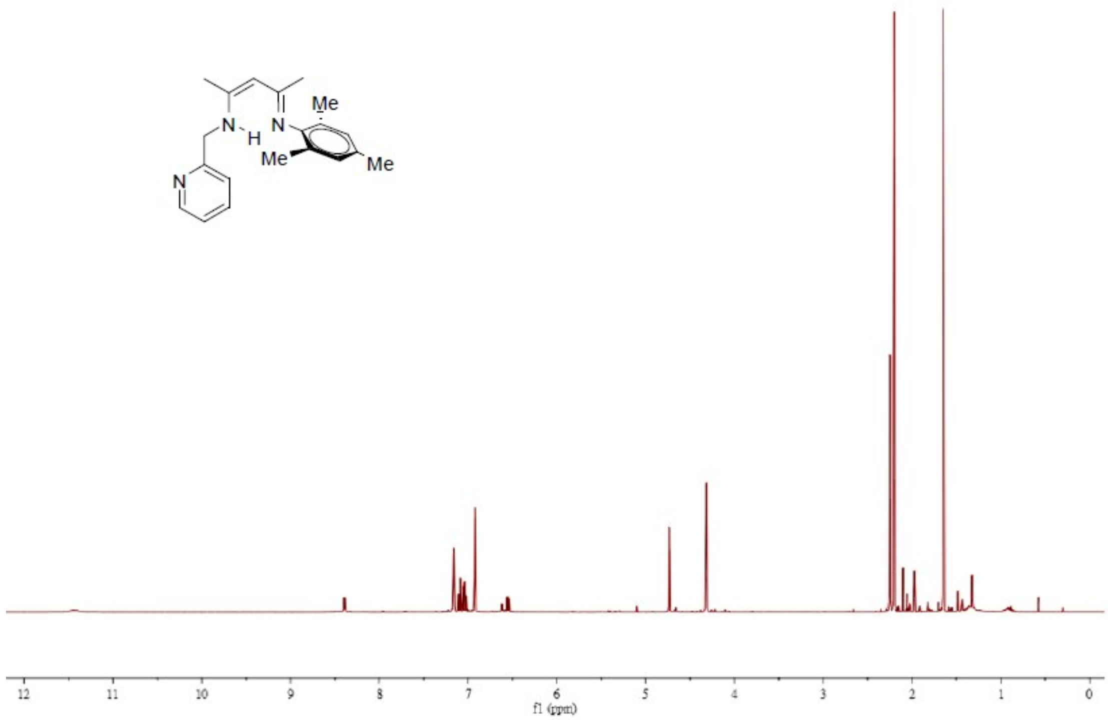

Figure S1. ^{1}H NMR spectrum of H**L¹** in C_6D_6 (400 MHz).

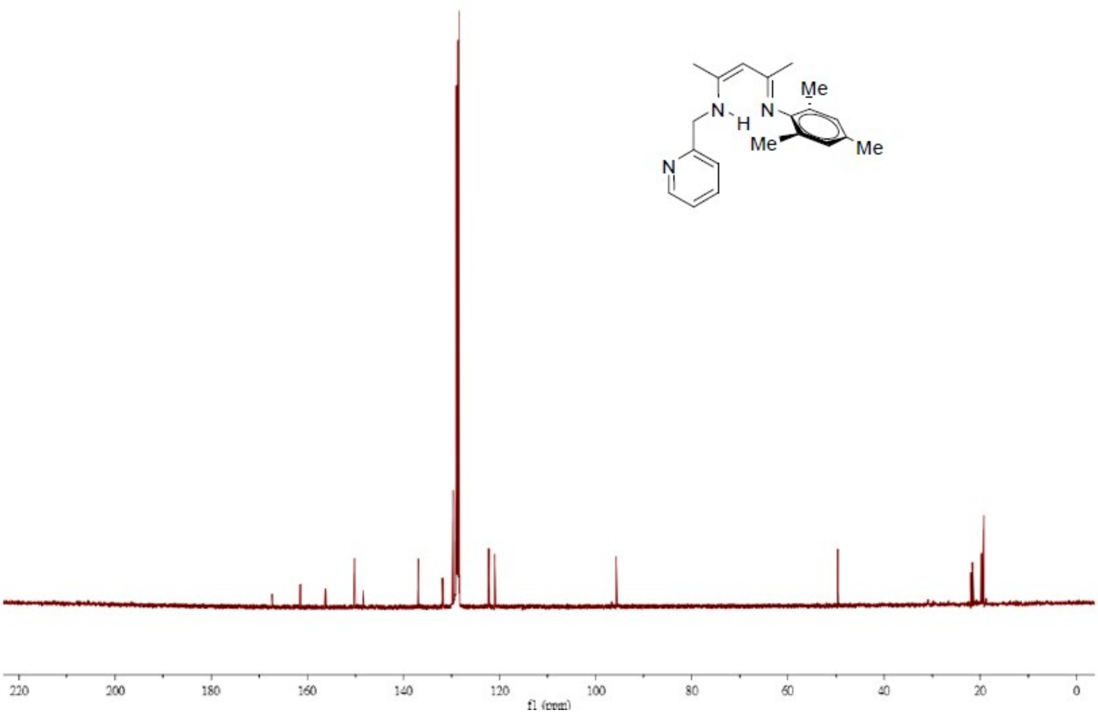

Figure S2. $^{13}C\{^{1}H\}$ NMR spectrum of H**L¹** in C_6D_6 (100 MHz).

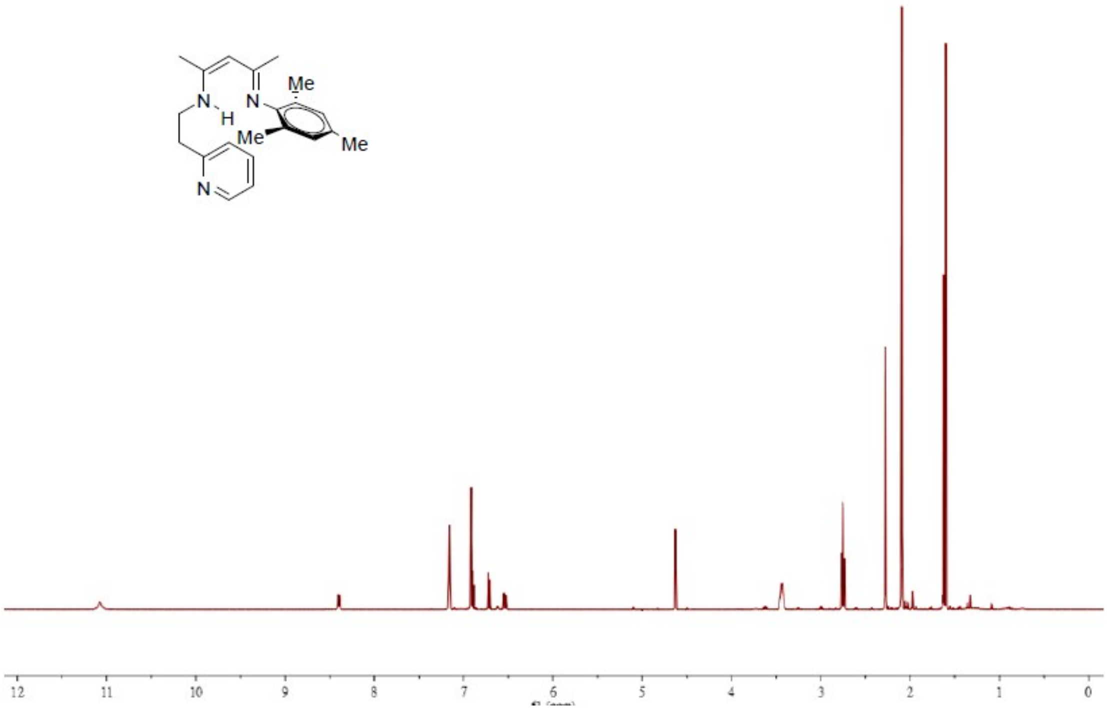

Figure S3. ^{1}H NMR spectrum of H**L^{2}** in C_6D_6 (400 MHz).

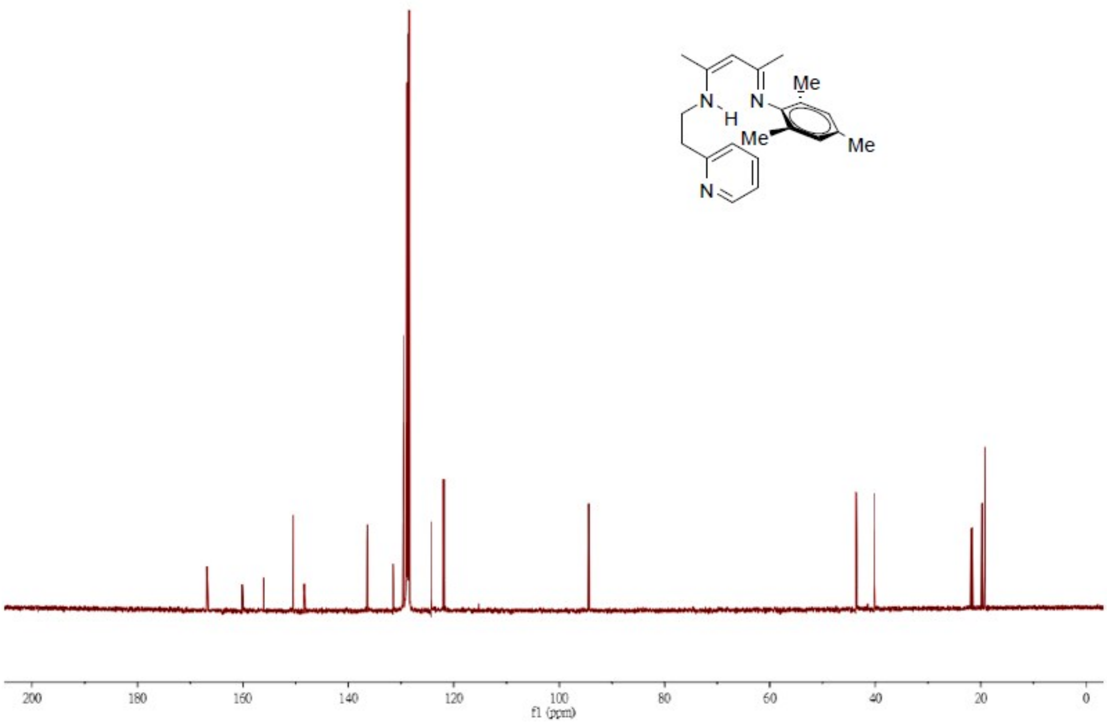

Figure S4. ^{13}C {^{1}H } NMR spectrum of H**L^{2}** in C_6D_6 (100 MHz).

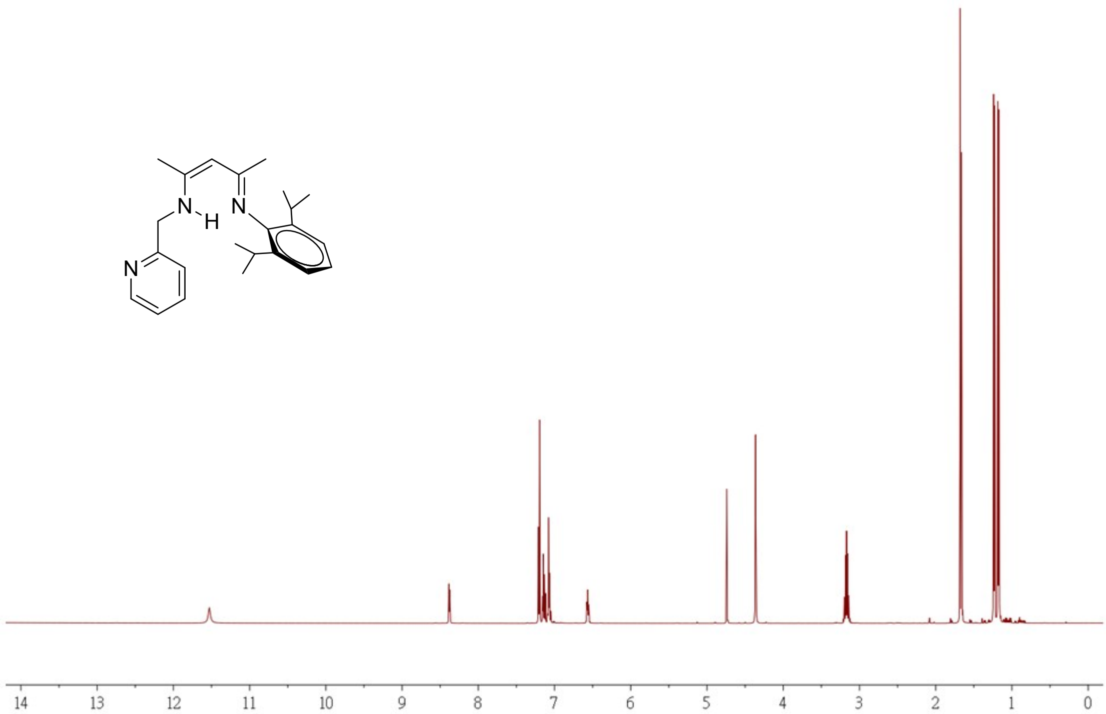

Figure S5. ^{1}H NMR spectrum of H**L^{3}** in C_6D_6 (500 MHz).

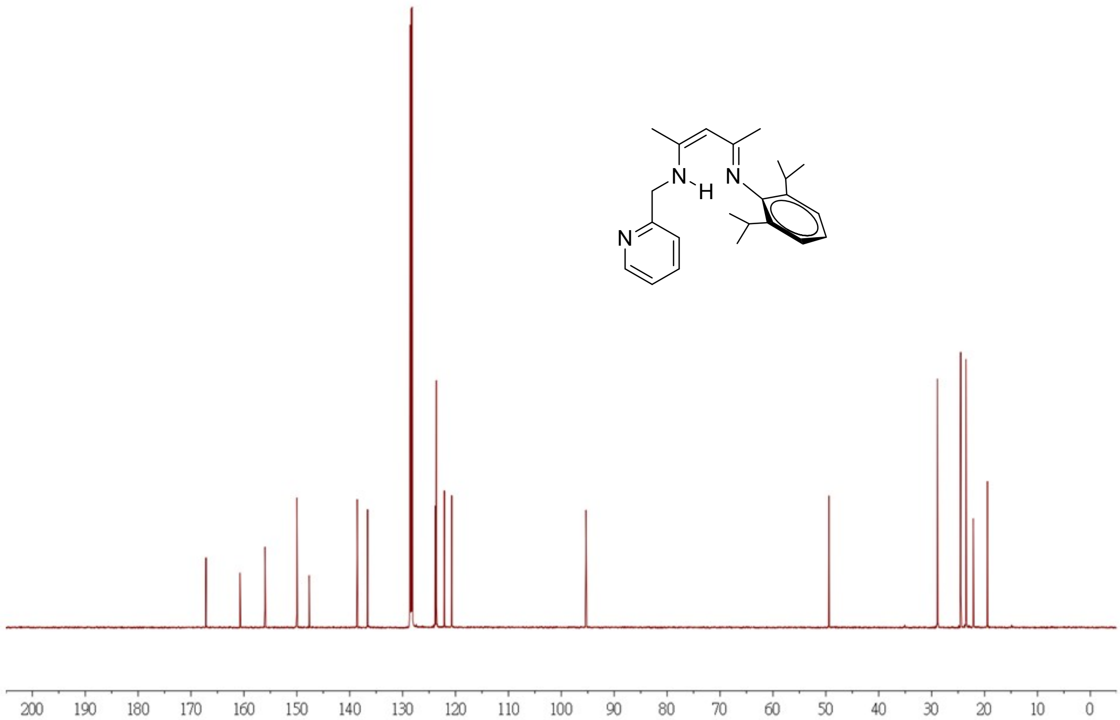

Figure S6. ^{13}C {^{1}H } NMR spectrum of H**L^{3}** in C_6D_6 (125 MHz).

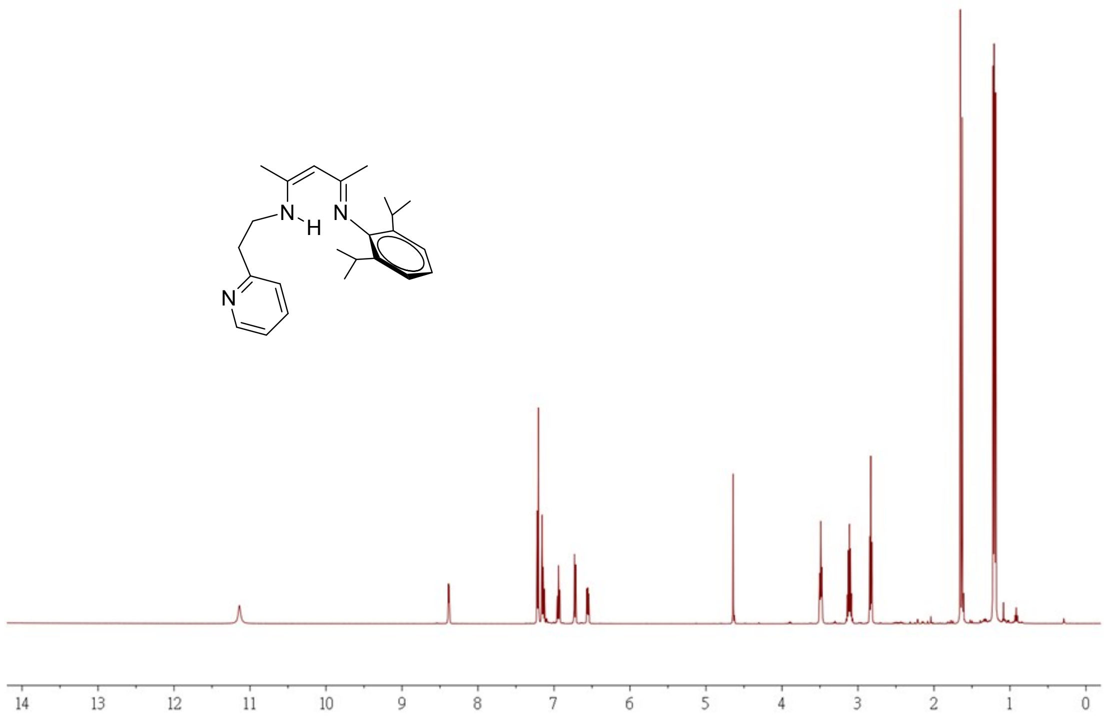

Figure S7. ^{1}H NMR spectrum of H**L**^{4} in C_6D_6 (500 MHz).

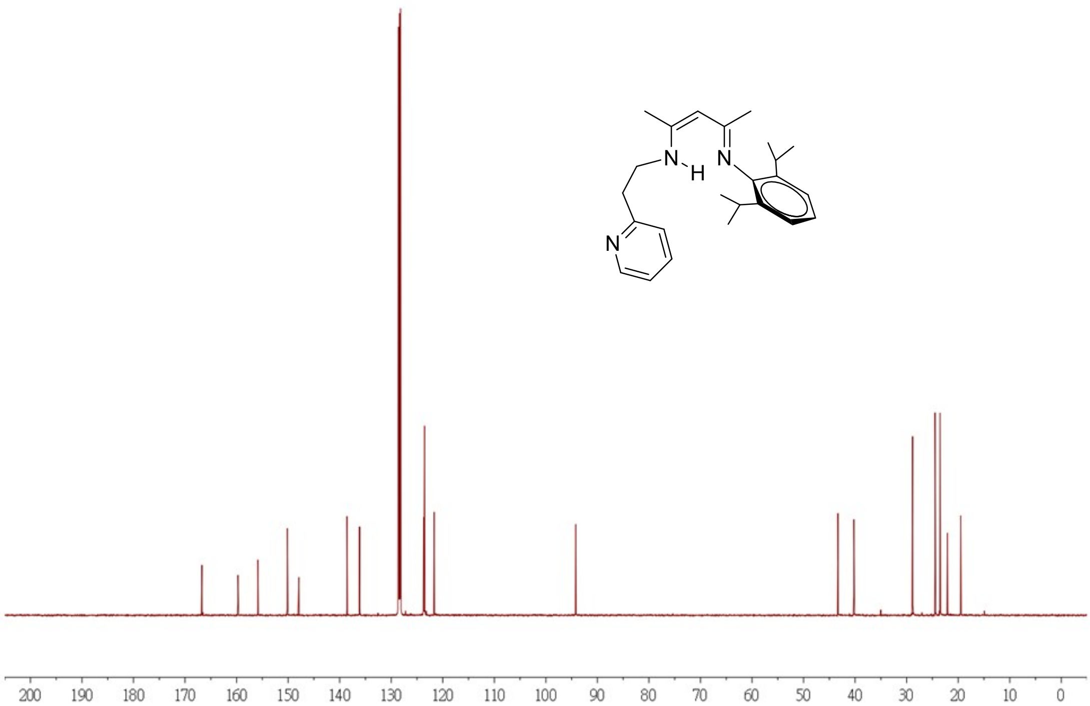

Figure S8. ^{13}C {^{1}H } NMR spectrum of H**L**^{4} in C_6D_6 (125 MHz).

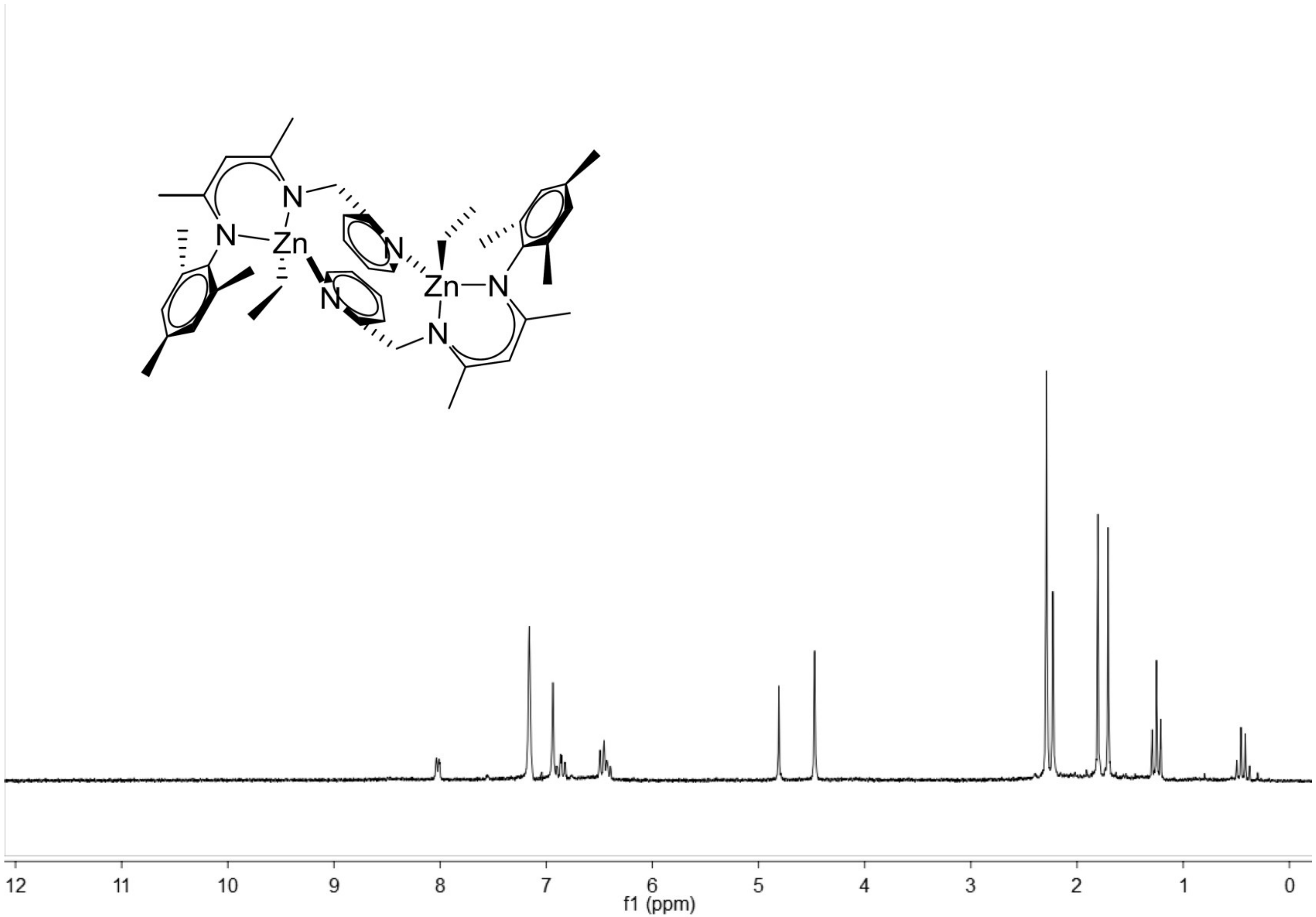

Figure S9. ^{1}H NMR spectrum of **1** in C_6D_6 (400 MHz).

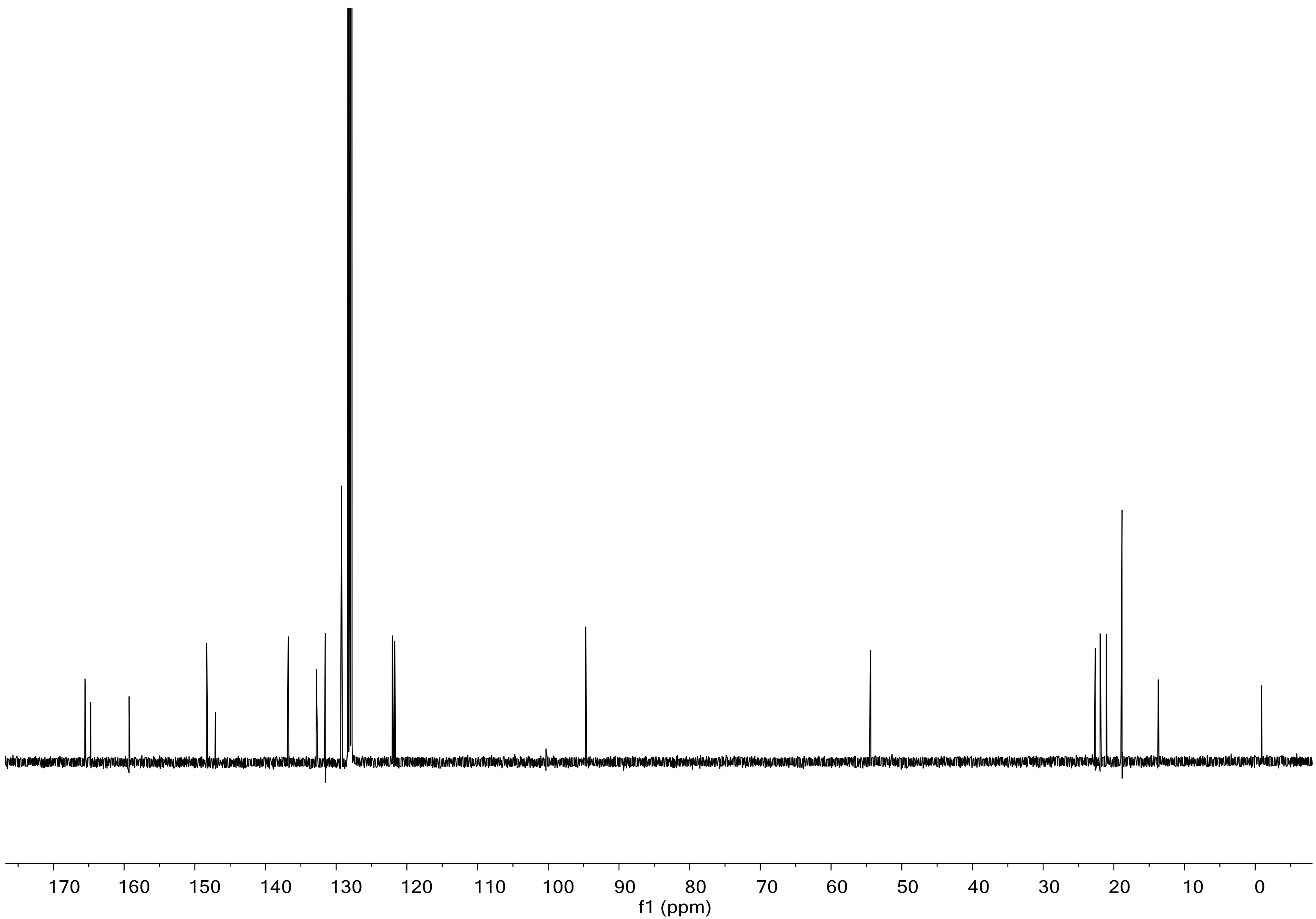

Figure S10. $^{13}C\ \{^{1}H\}$ NMR spectrum of **1** in C_6D_6 (100 MHz).

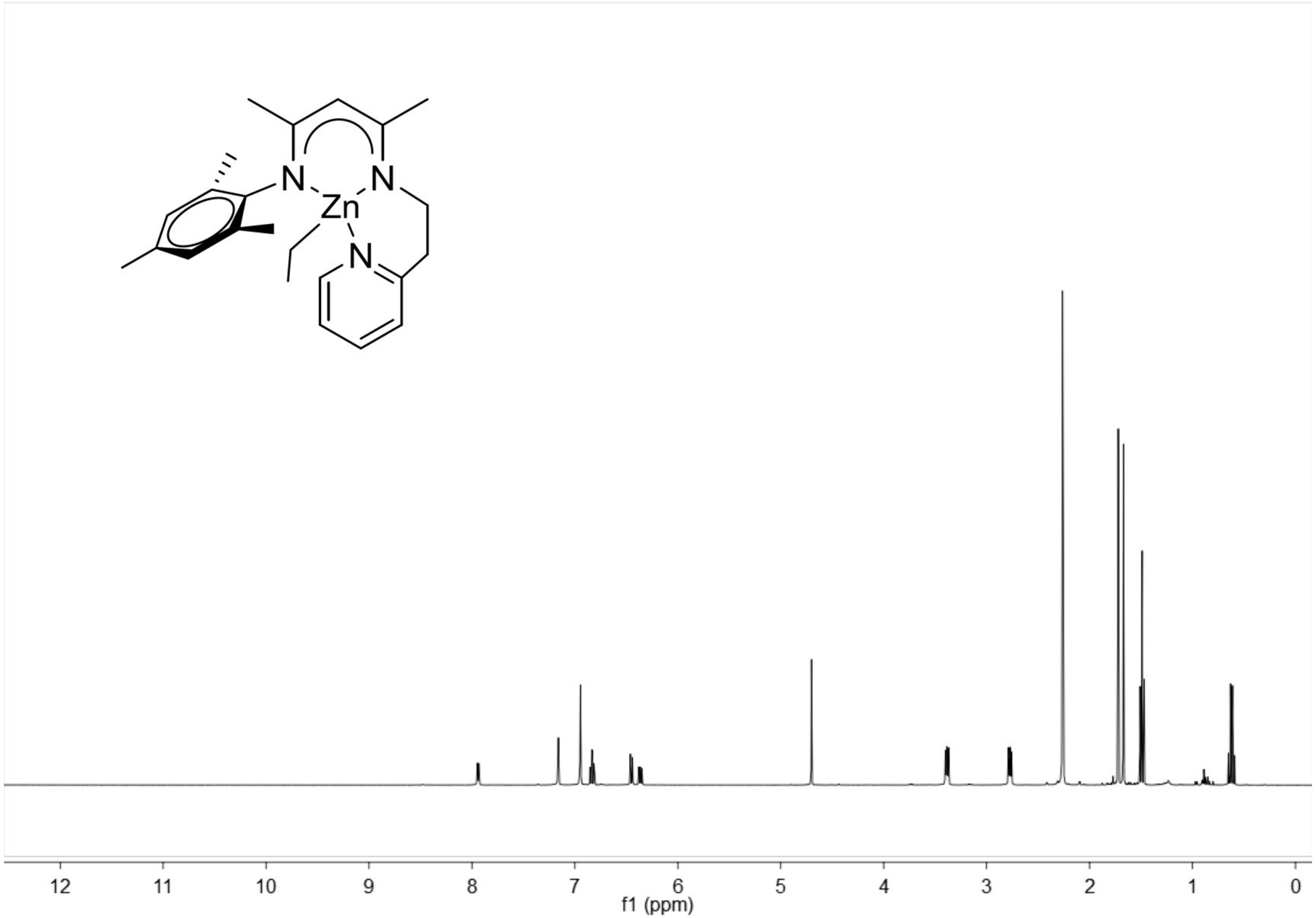

Figure S11. ^{1}H NMR spectrum of **2** in C_6D_6 (400 MHz).

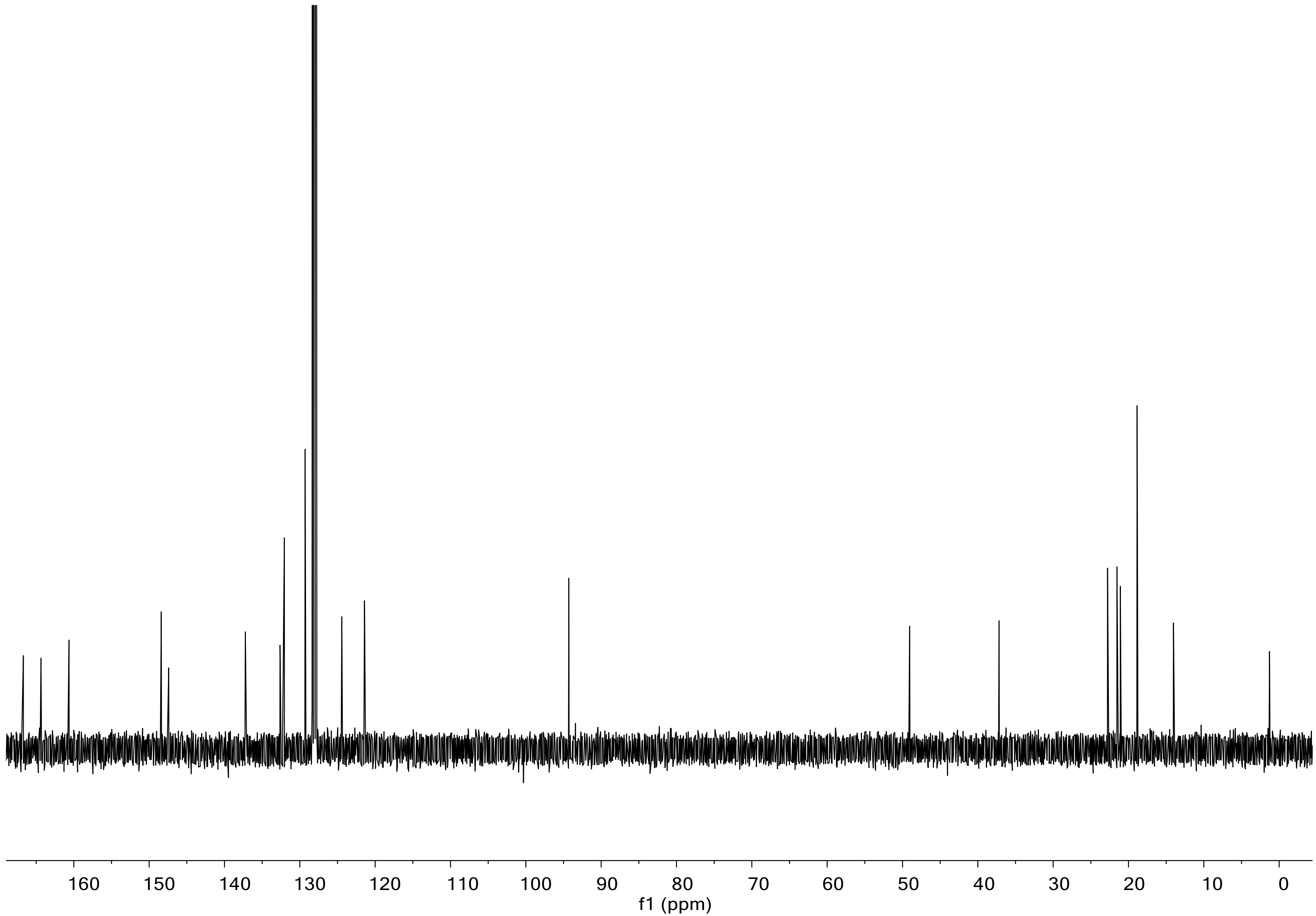

Figure S12. $^{13}C\{^{1}H\}$ NMR spectrum of **2** in C_6D_6 (100 MHz).

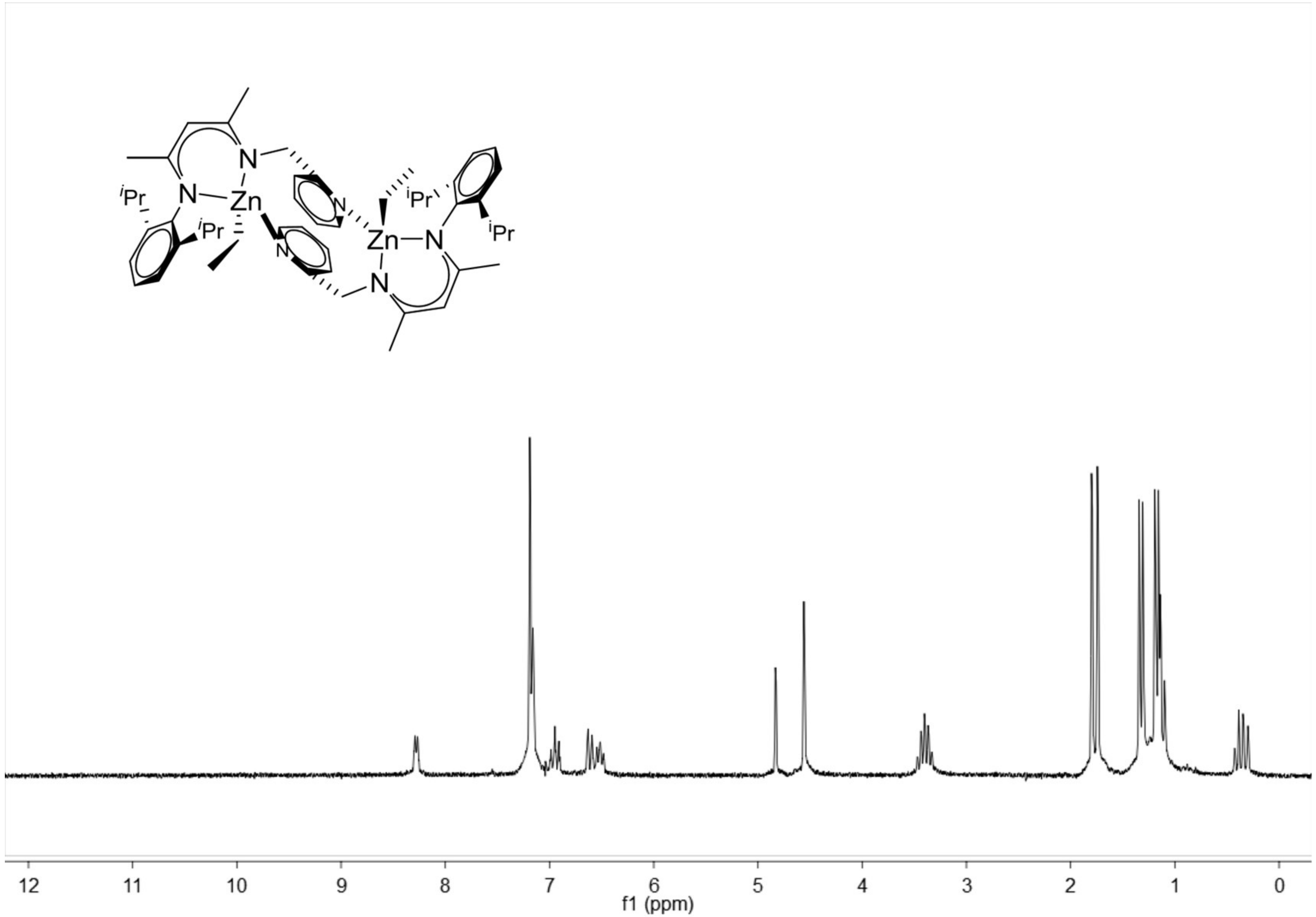

Figure S13. ^{1}H NMR spectrum of **3** in C_6D_6 (400 MHz).

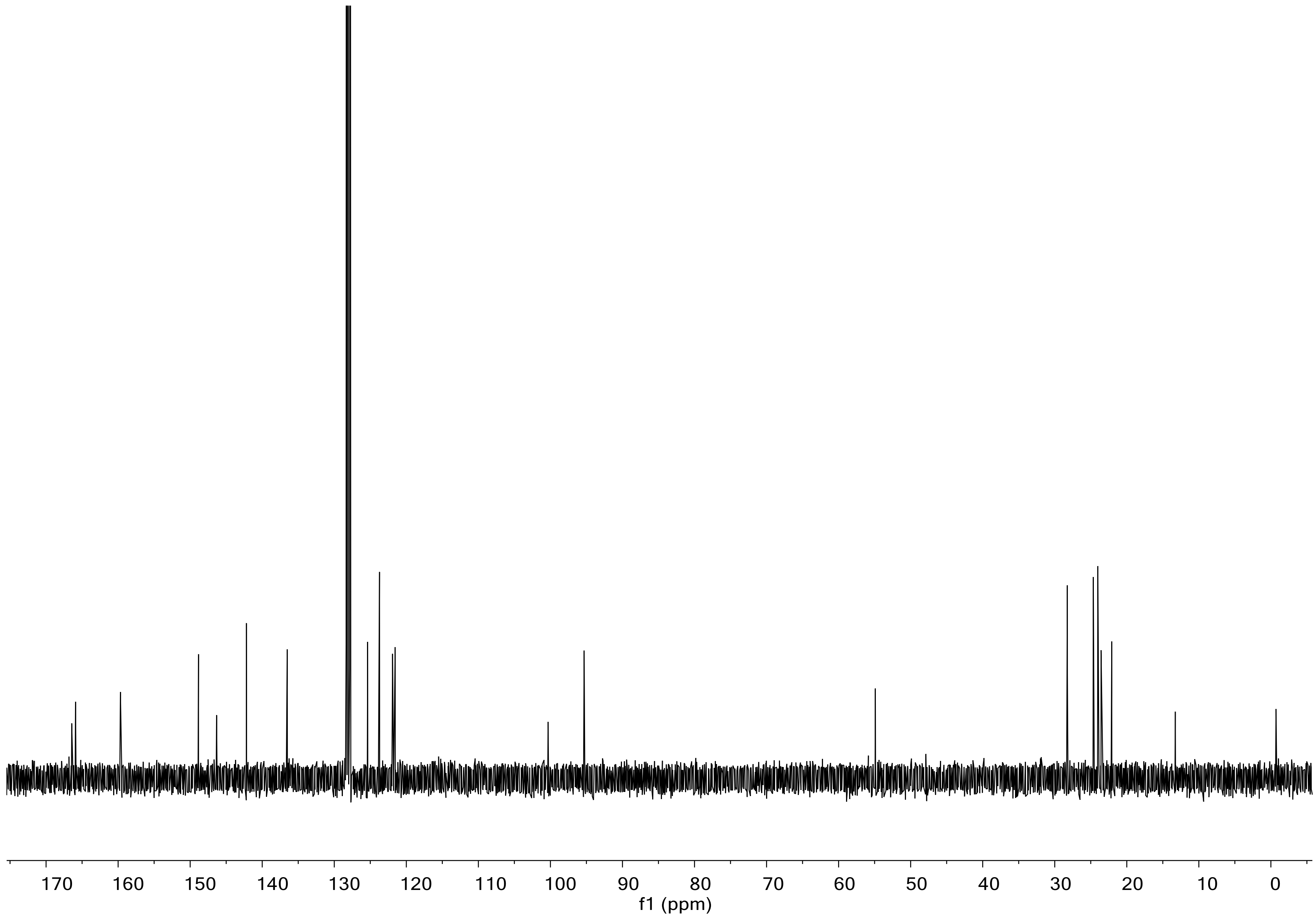

Figure S14. $^{13}C\{^1H\}$ NMR spectrum of **3** in C_6D_6 (100 MHz).

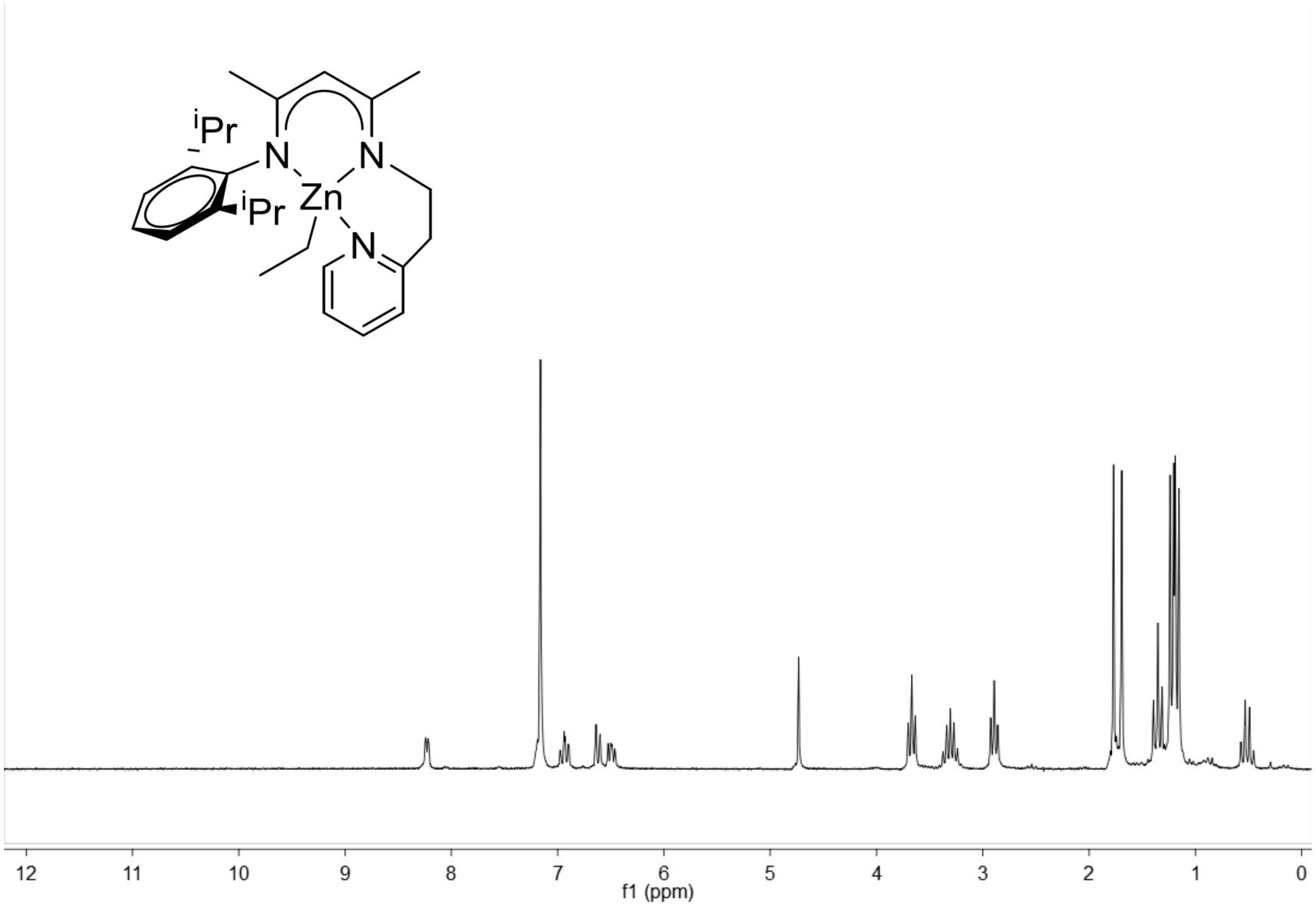

Figure S15. ^{1}H NMR spectrum of **4** in C_6D_6 (400 MHz).

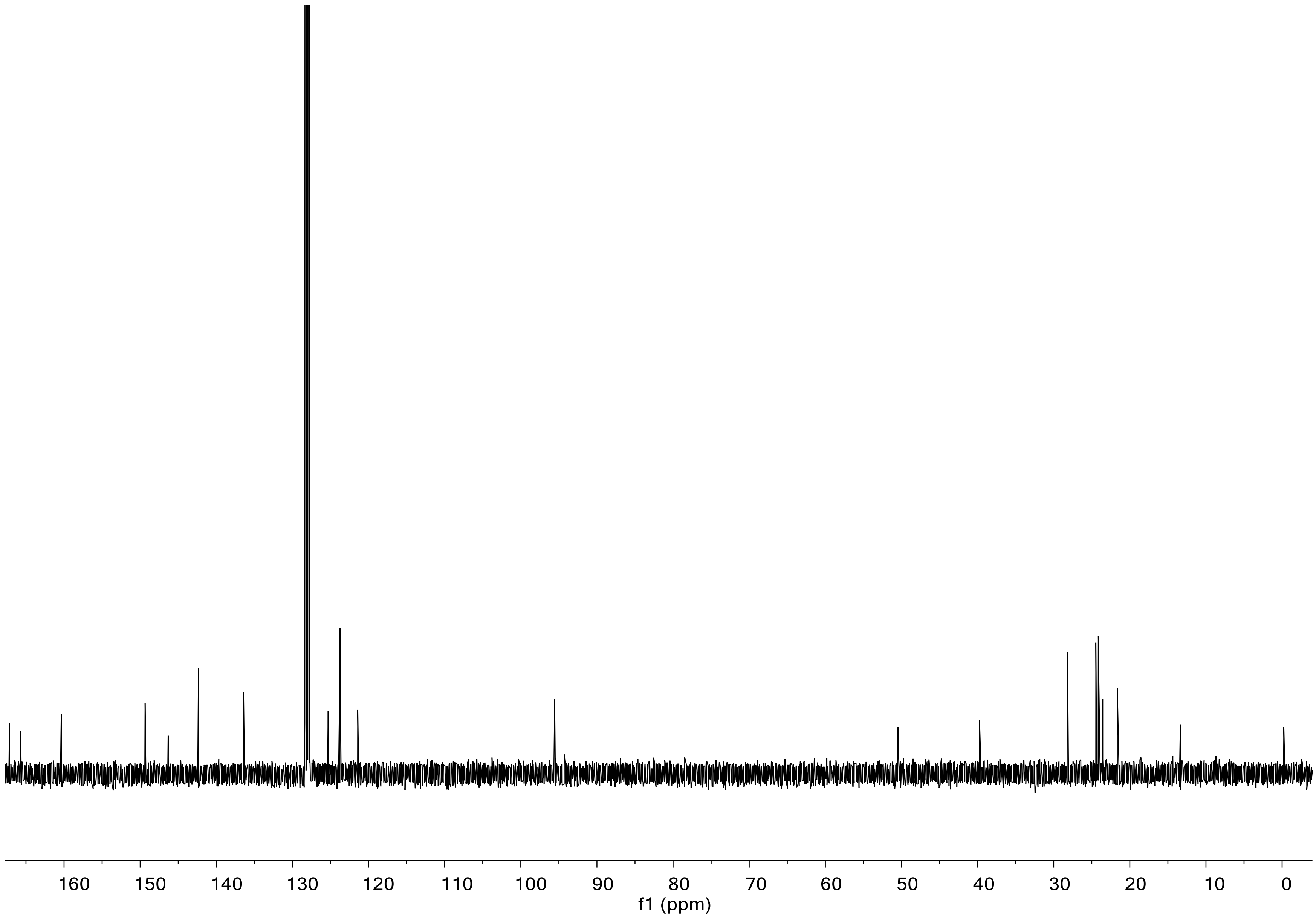

Figure S16. $^{13}C\ \{^{1}H\}$ NMR spectrum of **4** in C_6D_6 (100 MHz).

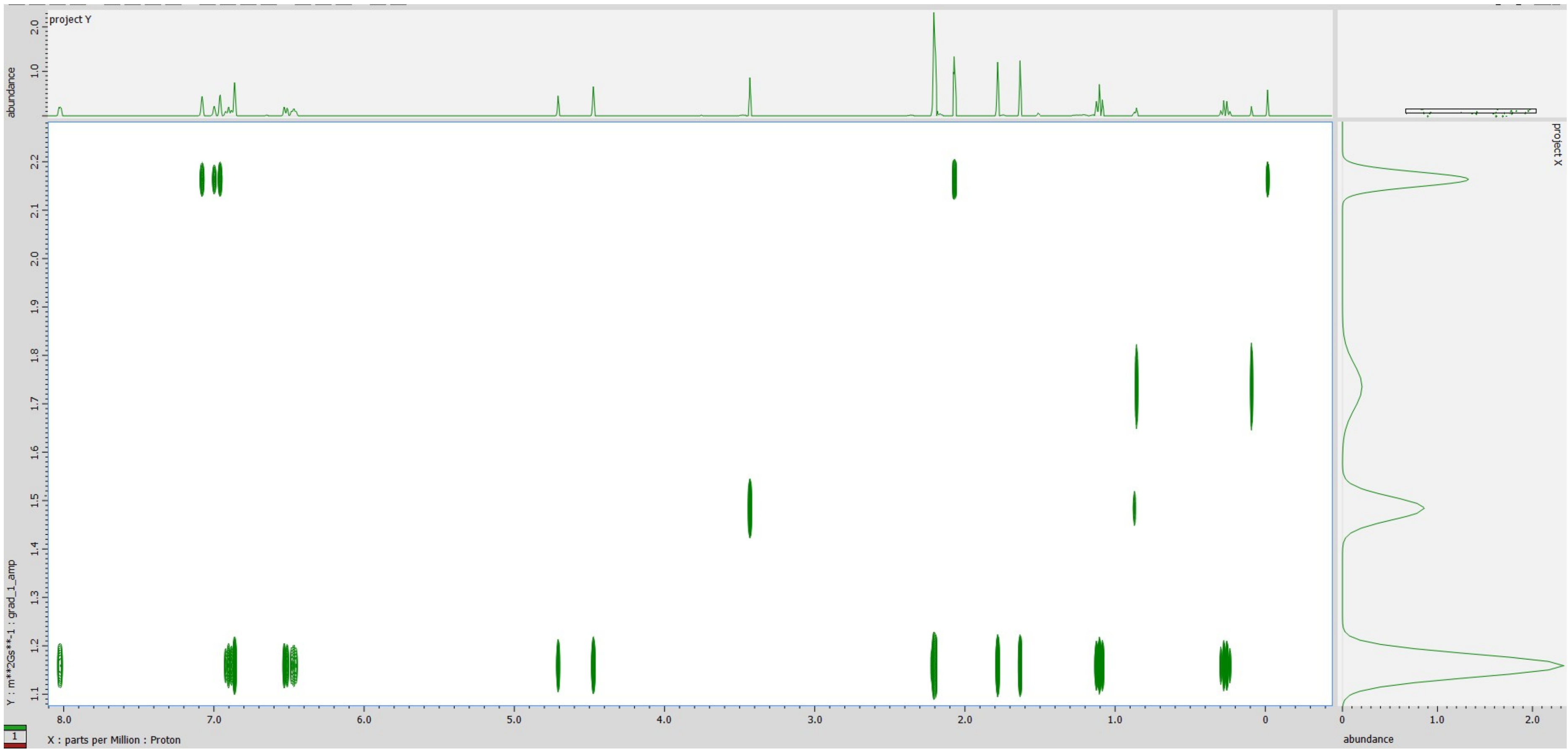

Figure S17. ^{1}H DOSY spectrum of **1** and three internal references in toluene-d8.

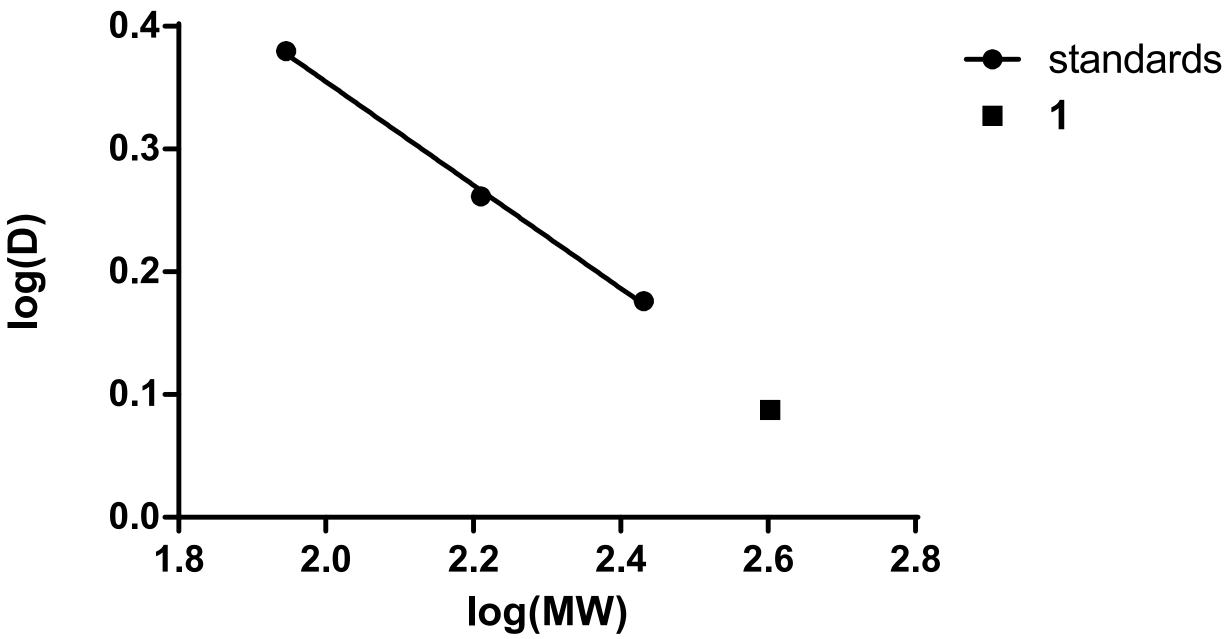

Equation	Y = -0.4207*X + 1.196
R square	0.9983
MW from eq.	431.84
ERROR	7.71%

Figure S18. D-FW analysis of ^{1}H DOSY data. Internal references are shown as solid circles and complex **1** is shown as solid square.

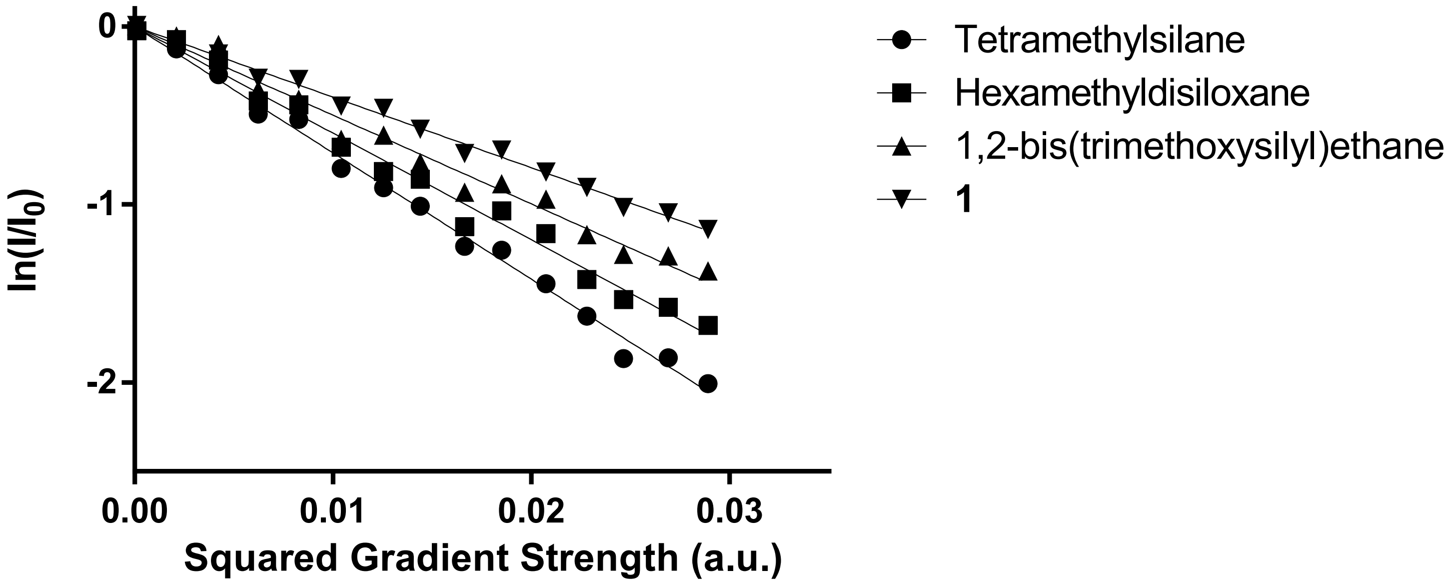

complex	Equation	R square
Tetramethylsilane	Y = -70.97*X - 0.0008717	0.9938
Hexamethyldisiloxane	Y = -59.93*X - 0.0004703	0.9867
1,2-bis(trimethoxysilyl)ethane	Y = -49.83*X - 0.0006224	0.9802
1	Y = -39.69*X - 0.0004944	0.9935

Figure S19. Stejskal-Tanner plot of experimental peaks for complex **1** and their best fit lines.

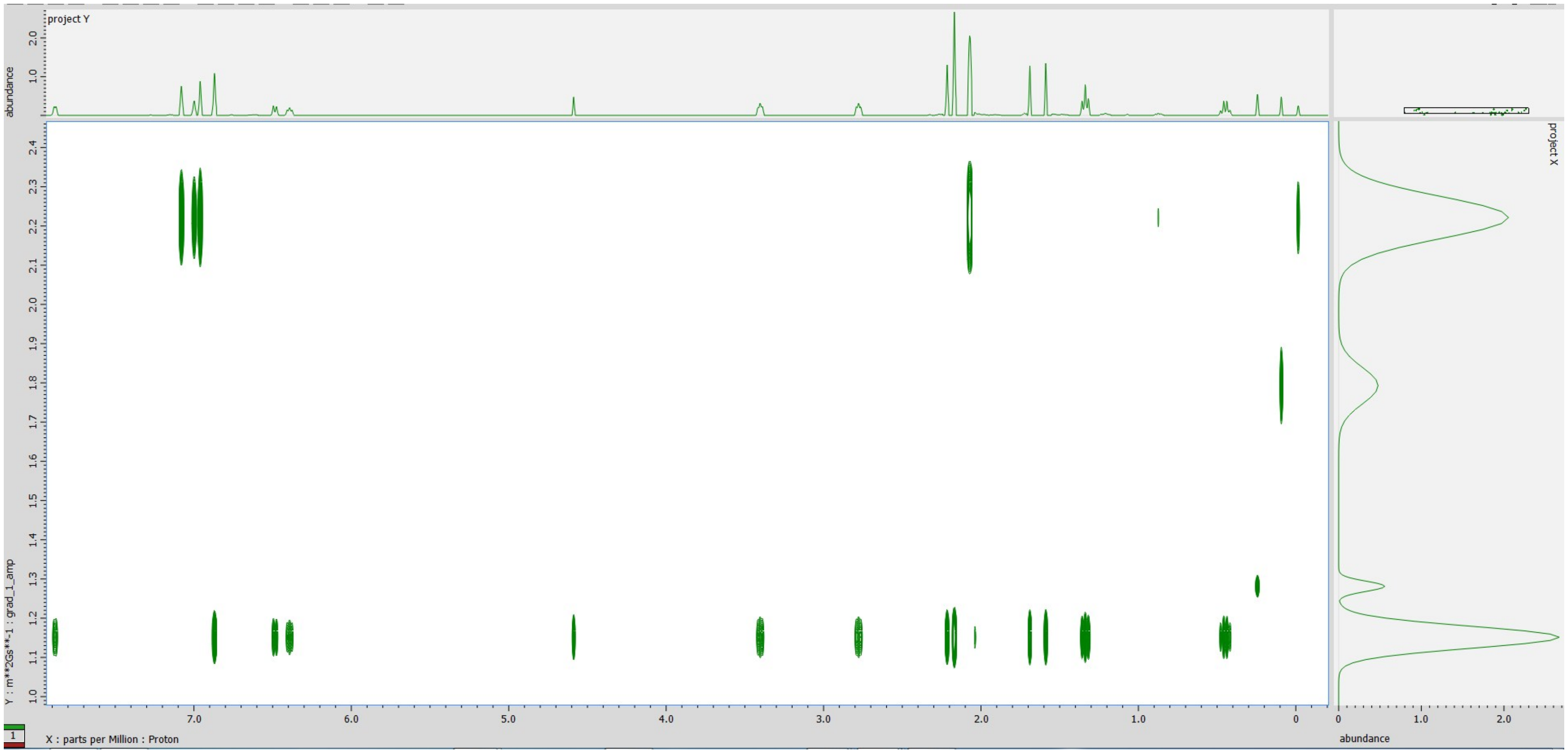

Figure S20. ^{1}H DOSY spectrum of **2** and three internal references in toluene-d8.

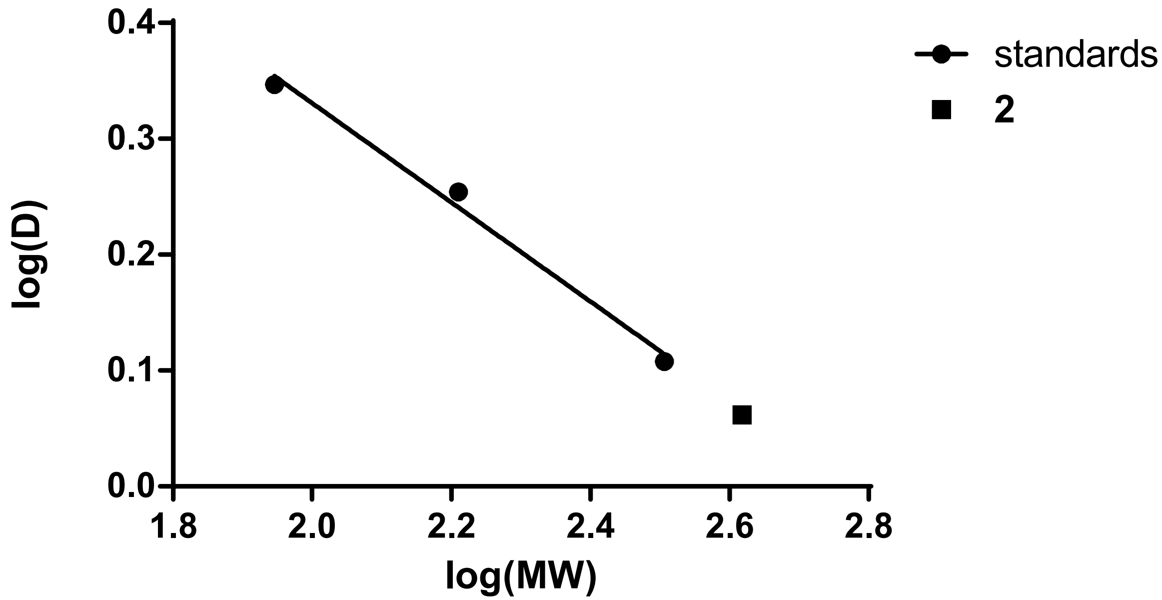

Equation	Y = -0.4278*X + 1.186
R square	0.9907
MW from eq.	425.09
ERROR	2.45%

Figure S21. D-FW analysis of ^{1}H DOSY data. Internal references are shown as solid circles and complex **2** is shown as solid square.

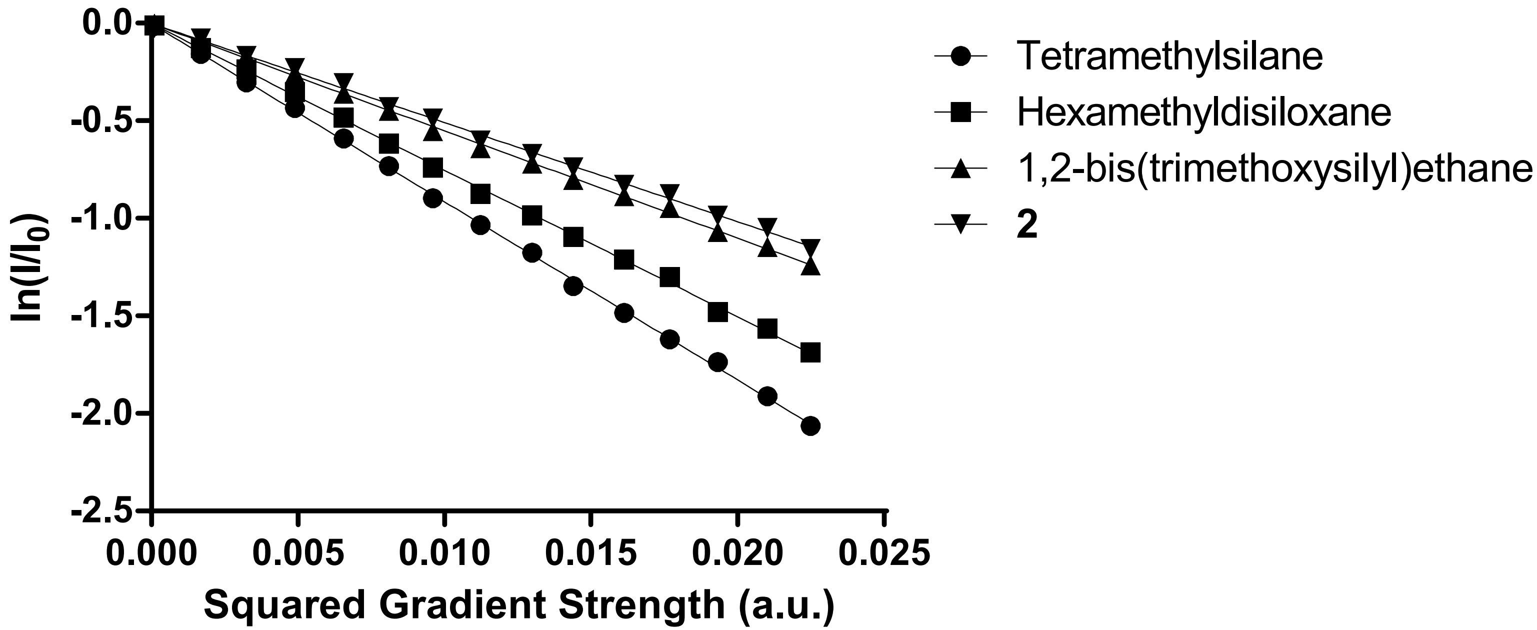

complex	Equation	R square
Tetramethylsilane	Y = -91.24*X - 0.002636	0.9995
Hexamethyldisiloxane	Y = -75.13*X - 0.002174	0.9991
1,2-bis(trimethoxysilyl)ethane	Y = -54.98*X - 0.001595	0.9989
1	Y = -50.78*X - 0.001481	0.9978

Figure S22. Stejskal-Tanner plot of experimental peaks for complex **2** and their best fit lines.

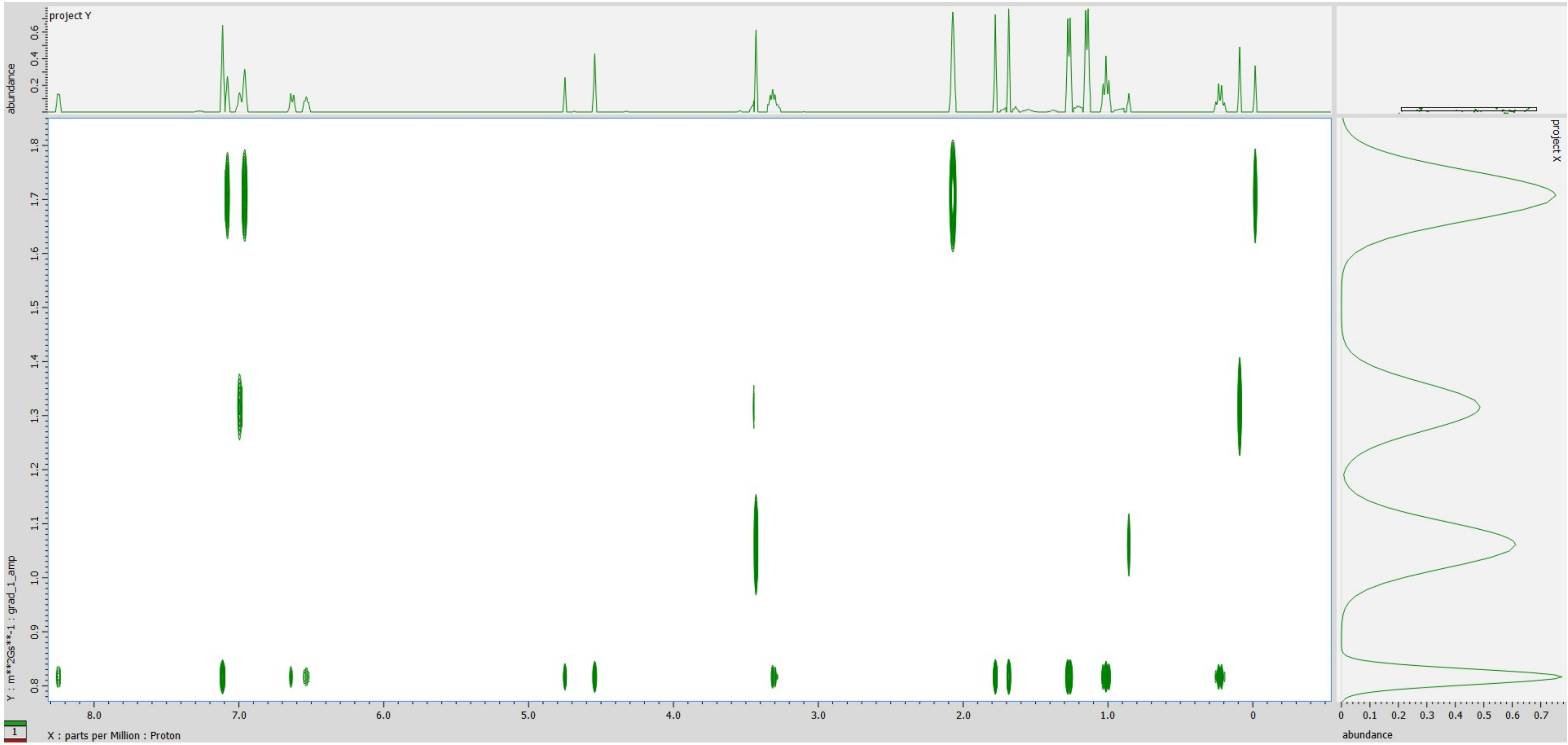

Figure S23. [1]H DOSY spectrum of complex **3** and three internal references in toluene-d8.

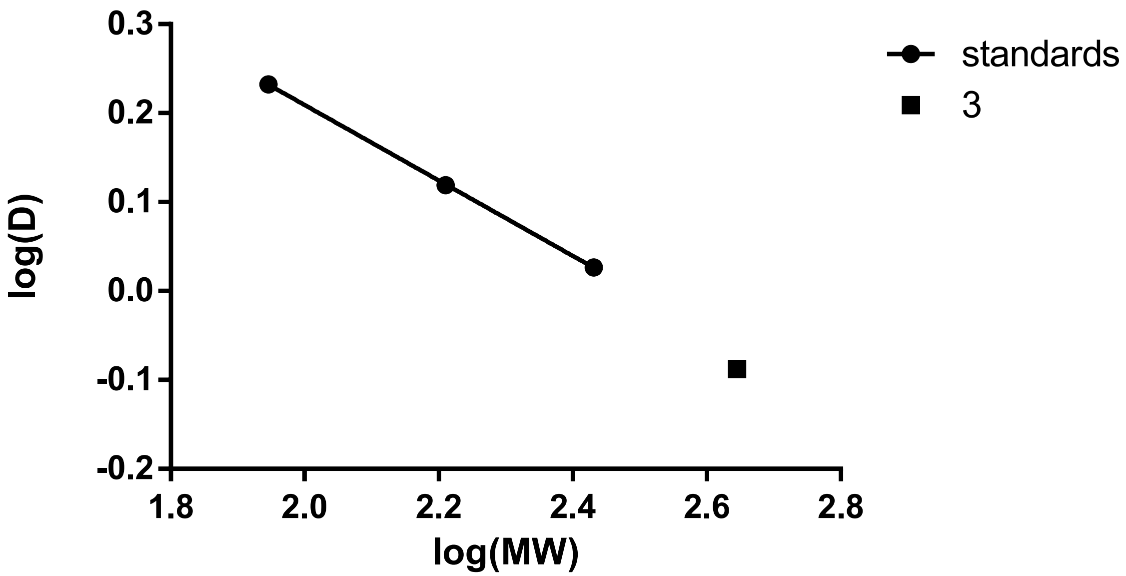

Equation	Y = -0.4240*X + 1.057
R square	1.000
MW from eq.	501.17
ERROR	13.4%

Figure S24. D-FW analysis of ^{1}H DOSY data. Internal references are shown as solid circles and complex **3** is shown as solid square.

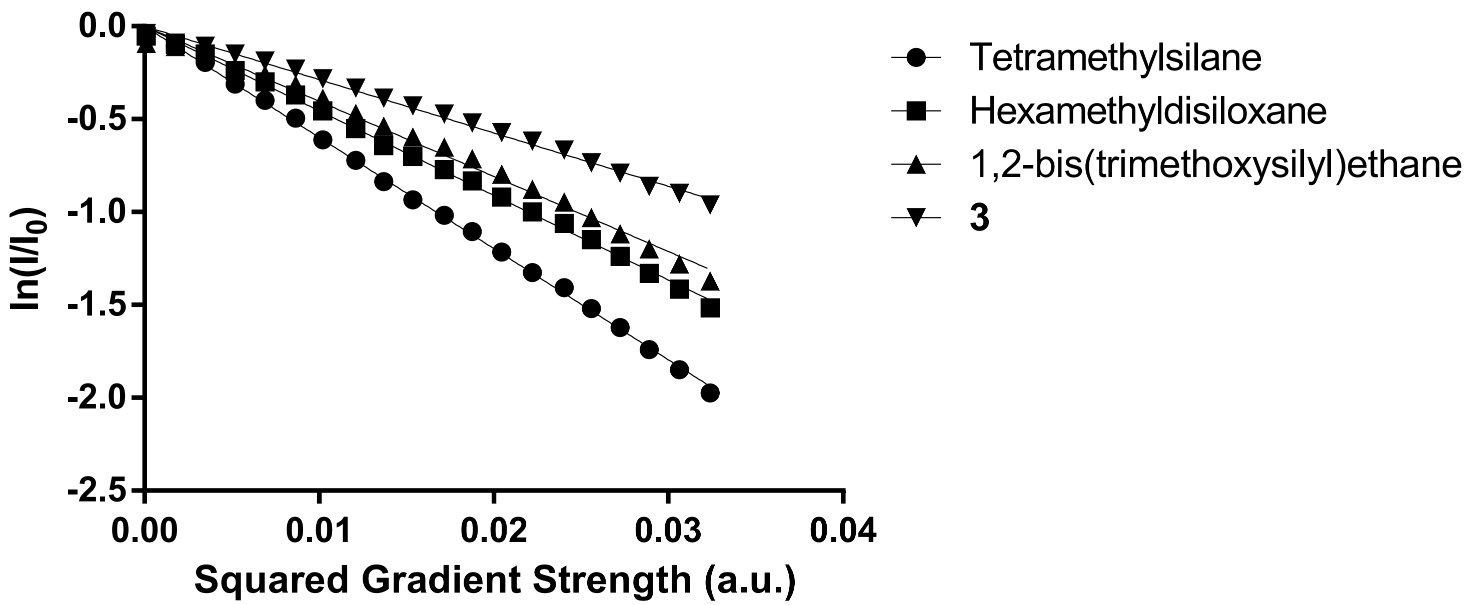

complex	Equation	R square
Tetramethylsilane	Y = -59.86*X + 0.0001005	0.9990
Hexamethyldisiloxane	Y = -45.52*X + 6.586e-005	0.9979
1,2-bis(trimethoxysilyl)ethane	Y = -40.42*X + 5.689e-006	0.9921
3	Y = -28.71*X - 3.200e-005	0.9946

Figure S25. Stejskal-Tanner plot of experimental peaks for complex **3** and their best fit lines.

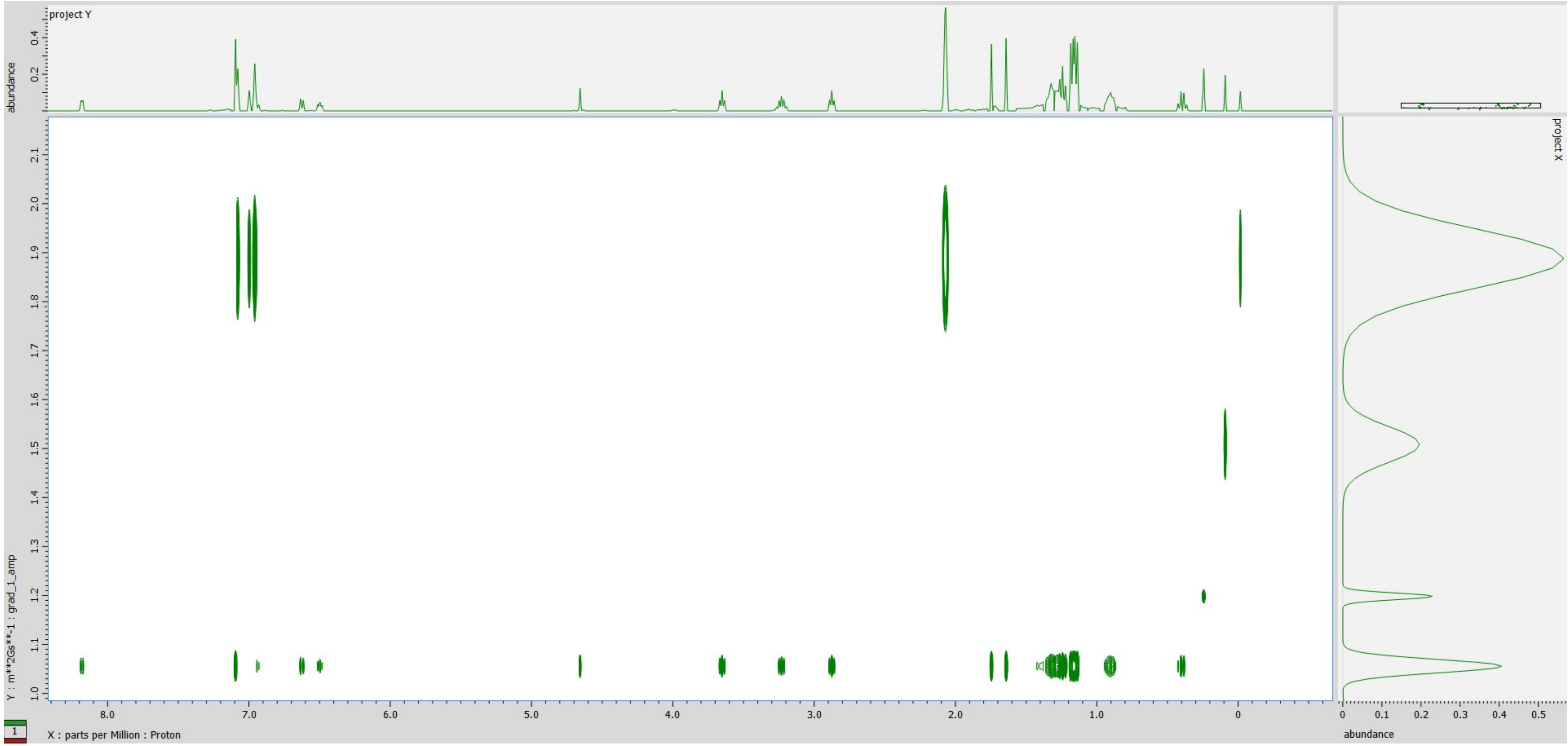

Figure S26. ^{1}H DOSY spectrum of complex **4** and three internal references in toluene-d8.

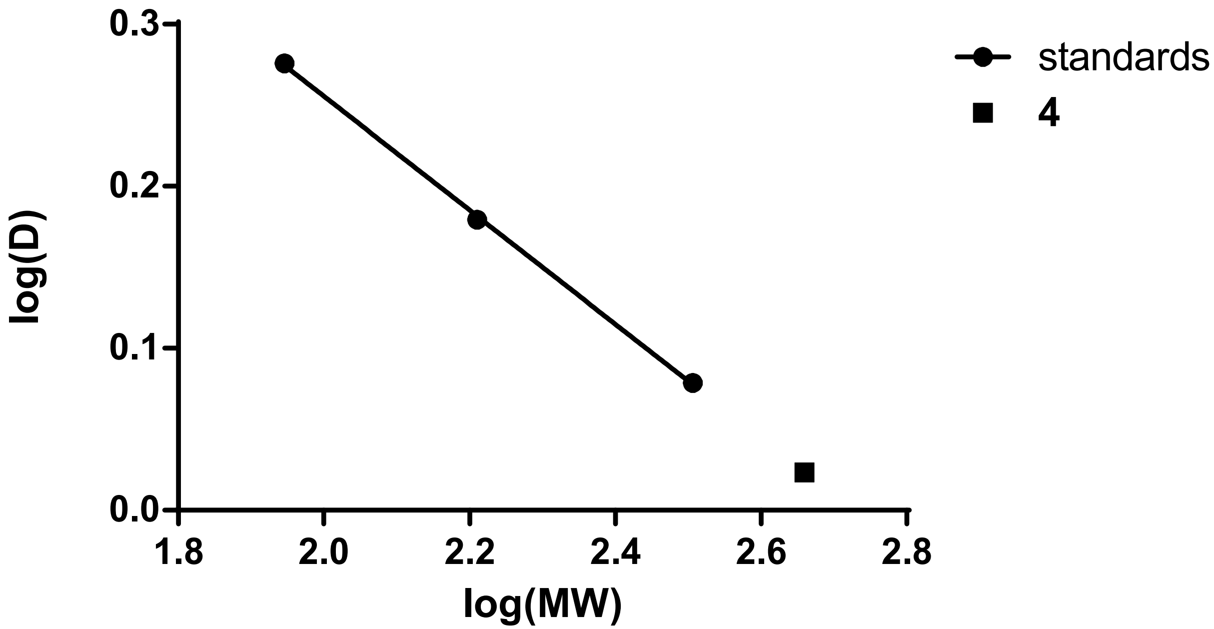

Equation	Y = -0.3516*X + 0.9588
R square	0.9996
MW from eq.	457.78
ERROR	2.33%

Figure S27. D-FW analysis of ^{1}H DOSY data. Internal references are shown as solid circles and complex **4** is shown as solid square.

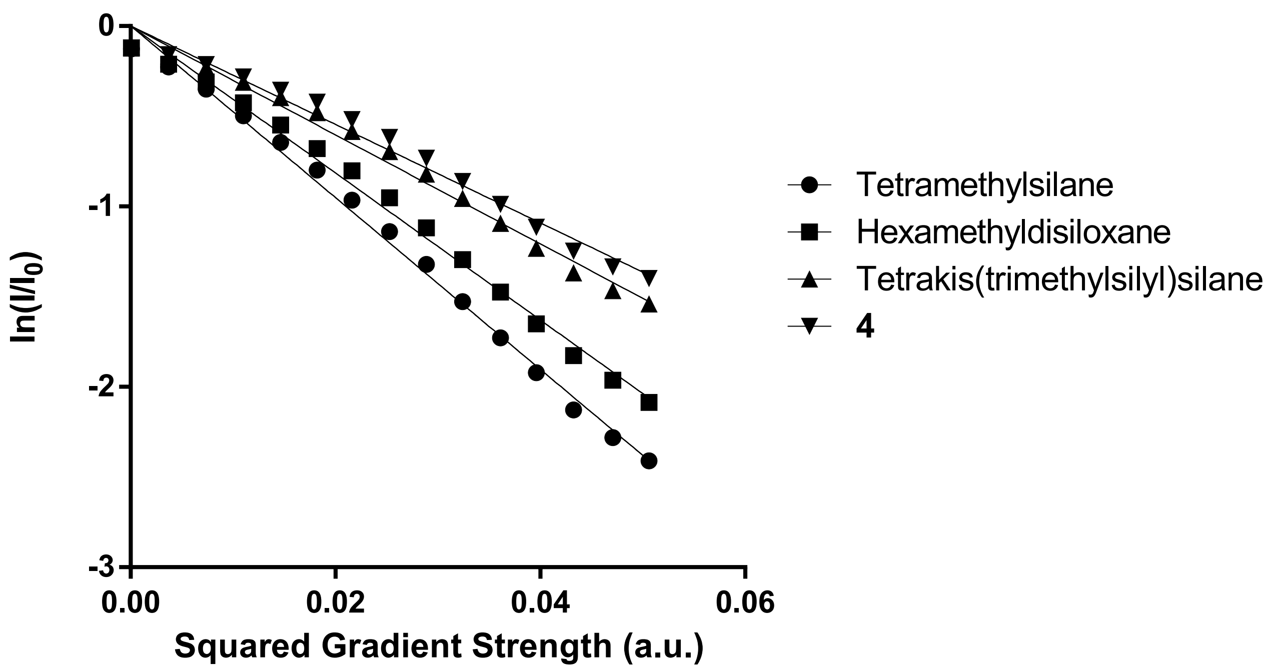

complex	Equation	R square
Tetramethylsilane	Y = -47.62*X + 0.002039	0.9946
Hexamethyldisiloxane	Y = -40.77*X + 0.001773	0.9920
1,2-bis(trimethoxysilyl)ethane	Y = -30.20*X + 0.001304	0.9873
4	Y = -27.30*X + 0.001206	0.9825

Figure S28. Stejskal-Tanner plot of experimental peaks for complex **4** and their best fit lines.

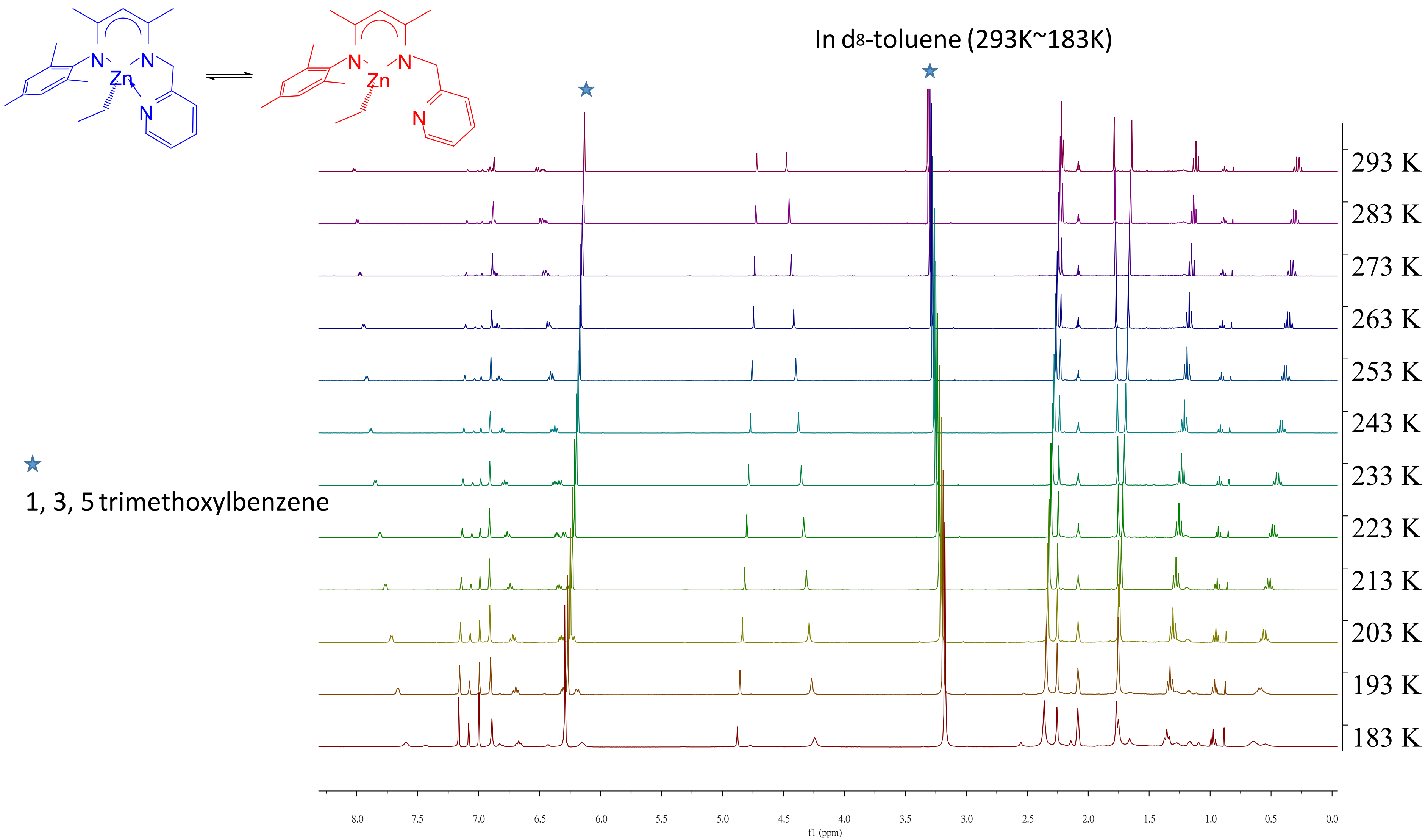

Figure S29. Variable Temperature ^{1}H NMR experiment of complex **1** (293K~183K)

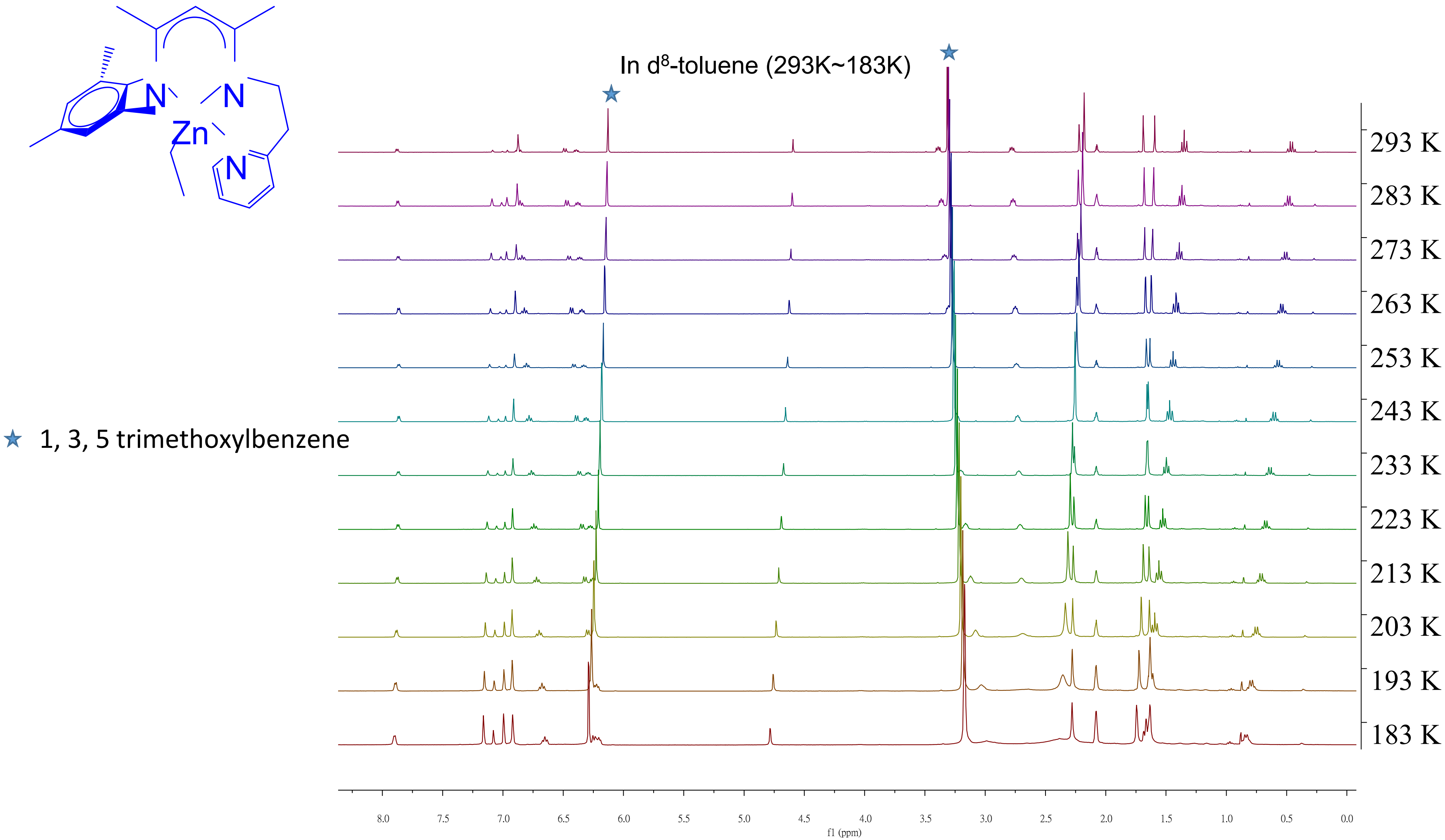

Figure S30. Variable Temperature ^{1}H NMR experiment of complex **2** (293K~183K)